Synthetic microparticles conjugated with $VEGF_{165}$ improve the survival and function of endothelial progenitor cells *via* microRNA-17 inhibition

Sezin Aday[1,2,3,4], Janet Zoldan[5], Marie Besnier[4], Laura Carreto[6], Jaimy Saif[4], Rui Fernandes[7], Tiago Santos[8], Liliana Bernardino[8], Robert Langer[3], Costanza Emanueli[4,9,#], Lino Ferreira[1,2,#]

[1]CNC-Center for Neuroscience and Cell Biology, University of Coimbra, 3004-517, Coimbra, Portugal,
[2]Faculty of Medicine, University of Coimbra, 3000-548, Coimbra, Portugal,
[3]Department of Chemical Engineering, Massachusetts Institute of Technology, Cambridge, MA 02139, USA,
[4]Bristol Heart Institute, School of Clinical Sciences, University of Bristol, BS2 8HW, England, UK,
[5]Department of Biomedical Engineering, Cockrell School of Engineering, The University of Texas at Austin, TX 78712, USA,
[6]University of Aveiro, 3810-193, Aveiro, Portugal,
[7]HEMS - Histology and Electron Microscopy Service, IBMC / I3S, Universidade do Porto, 4200-135 Porto, Portugal,
[8]Health Sciences Research Centre, Faculty of Health Sciences, University of Beira Interior, 6201-506, Covilhã, Portugal
[9]National Heart and Lung Institute, Hammersmith Campus, Imperial College of London, London, SW7 2AZ, England, UK.

[#]Corresponding authors:
Lino Ferreira
Center for Neuroscience and Cell Biology, University of Coimbra, 3004-517 Coimbra
Phone: +351 231 419 040
E-mail: lino@uc-biotech.pt

Costanza Emanueli
University of Bristol, School of Clinical Sciences, Bristol Royal Infirmary Level 7, Upper Maudlin Street, Bristol, BS2 8HW 39, England, UK
Phone: +44 0117 342 351 231
Email: Costanza.Emanueli@bristol.ac.uk

Abstract

Several cell-based therapies are under pre-clinical and clinical evaluation for the treatment of ischemic diseases. Poor survival and vascular engraftment rates of transplanted cells force them to work mainly via time-limited paracrine actions. Although several approaches, including the use of soluble $VEGF_{165}$ (sVEGF), have been developed in the last 10 years to enhance cell survival, they showed limited efficacy. Here, we report a pro-survival approach based on VEGF-immobilized microparticles (VEGF-MPs). VEGF-MPs prolonged VEGFR-2 and Akt phosphorylation in cord blood-derived late outgrowth endothelial progenitor cells (OEPCs). *In vivo*, OEPC aggregates containing VEGF-MPs showed higher survival than those treated with sVEGF. Additionally, VEGF-MPs decreased miR-17 expression in OEPCs, thus, increased the expression of its target genes *CDKN1A* and *ZNF652*. The therapeutic effect of OEPCs was improved *in vivo* by inhibiting miR-17. Overall, our data show a new experimental approach to improve therapeutic efficacy of proangiogenic cells for the treatment of ischemic diseases.

Keywords: Umbilical cord blood-derived endothelial progenitor cells; immobilized VEGF; synthetic microparticles; ischemia; microRNA-17.

Ischemic diseases are a leading cause of morbidity and mortality in the contemporary world. Several pre-clinical and clinical trials are exploring the therapeutic effect of cell-based therapies, in particular, bone marrow-derived proangiogenic cells and mesenchymal stem cells in ischemic diseases[1-3]. Unfortunately, most of the cells (more than 80%) die a few days (< 3 days) after delivery[4-6], thus hindering the therapeutic effect. Some approaches have been explored to augment cell survival in ischemic conditions. These include the exposure of transplanted cells to temperature shock, genetic modification of cells to overexpress growth factors and/or anti-apoptotic proteins and pre-conditioning the cells with pharmacological agents and cytokines[7, 8]. However, most of these methodologies have not reached the clinical trials, because they have shown limited effectiveness due to the multi-factorial nature of cell death. In addition, some of them are not cost-effective (e.g. recombinant proteins) or are difficult to implement from a regulatory standpoint (e.g. genetic modifications).

Vascular endothelial growth factor 165 (from now on referred as VEGF) is one of the most powerful and well-studied pro-survival/pro-angiogenic factors[9, 10]. Three main tyrosine kinase receptors initiate signal transduction cascades in response to soluble VEGF, including VEGF receptor 1 (VEGFR-1), VEGFR-2 and VEGFR-3[10, 11]. VEGF exerts its pro-survival effect mostly via VEGFR-2 by inducing its dimerization and subsequent phosphorylation of the receptor[12]. Although soluble and immobilized VEGF induce similar VEGF receptor phosphorylation, they have different properties[13]. In comparison to endothelial cells (ECs) cultured in the presence of soluble (free) VEGF (sVEGF), ECs cultured on VEGF-bound surfaces show different morphology[14], extended VEGFR-2 phosphorylation (mediated by the phosphorylation at the site Y1214 of the VEGFR-2 C-terminal tail)[13], and higher activation of the p38/MAPK pathway[13]. Due to the prolonged VEGFR-2 phosphorylation and higher activation of subsequent pathways, immobilized VEGF might be a promising pro-survival agent for cell-based therapies. However, the *in vitro* and *in vivo* pro-survival effects of

immobilized VEGF remain relatively elusive. In addition, the downstream molecular players mediating the biological effect of immobilized VEGF, particularly miRNAs, are still unknown.

Herein, we have engineered MPs with VEGF and studied the pro-survival effect and function of VEGF-MPs in OEPCs. We have additionally investigated the involvement of miRNAs in the biological responses to immobilized VEGF. Previous studies on the differential signaling responses of immobilized VEGF focused on planar surfaces that are not transplantable in most cases, thus making the identification of *in vivo* molecular players of immobilized VEGF difficult[13, 15]. Here, we have immobilized VEGF onto magnetic MPs of 4.5 μm, which can be assembled with OEPCs in cell aggregates and are transplantable. In this study, we have used $CD34^+$ cell-derived OEPCs[3]. In contrast to the "early" endothelial progenitor cells, OEPCs directly participate in tubulogenesis[16] and their neovasculogenesis properties have been demonstrated in pre-clinical tests using different animal models of hindlimb ischemia, diabetic chronic wounds, among others[4, 5, 17-19]. Moreover, although OEPCs express endothelial cell markers such as vWF, and VECAD; uptake acetylated LDL; and display the morphology of ECs, they show distinct features from mature ECs[6, 20].

We show that VEGF-MPs assembled into cell aggregates prolong the phosphorylation of VEGFR-2 and Akt in OEPCs in comparison to sVEGF. Furthermore, VEGF-MPs incorporated in cell aggregates increased OEPC survival both *in vitro* and *in vivo* as compared to cell aggregates, cell aggregates containing either uncoated MPs or sVEGF. We further show that the prolonged VEGFR-2 phosphorylation in cell aggregates containing VEGF-MPs is associated with a down-regulation of miR-17 and increase in the expression of its target genes *CDKN1A* and *ZNF652*.

The bioengineering platform used in this work opens a new avenue to improve the mechanistic understanding of how VEGF immobilization alters cell behaviors and what are the molecular mediators of this process, thus enabling the design of new therapies to treat ischemic diseases.

MATERIALS and METHODS

Extended protocols are available in the online only supplementary file. All microarray and sequencing data have been deposited into the Gene Express Omnibus public database (National Center for Biotechnology Information) under accession numbers GSE75899 (miRNA microarray) and GSE76663 (mRNA sequencing).

Preparation of VEGF-MPs. Histidine-tagged VEGF (his-VEGF; ProSpec-Tany TechnoGene Ltd., Ness-Ziona, Israel) was immobilized onto streptavidin-coated magnetic MPs conjugated with biotinylated anti-histidine antibody (R&D Systems, Minneapolis, MN, USA). Briefly, biotinylated anti-histidine antibody solution (1.5 μg per 10^6 particles) in 0.1% (w/v) BSA (Sigma-Aldrich, St. Louis, MO, USA) was mixed with a suspension of streptavidin-coated MPs at room temperature for 30 min under constant agitation. Magnetically removed MPs were then washed with PBS containing 0.1% BSA and resuspended in his-VEGF solution (500 μl; 4.5 μg in 0.1% BSA per 10^6 microparticles) at room temperature for 30 min under constant agitation. Following a second wash with PBS containing 0.1% BSA, conjugated MPs were stored in PBS at 4ºC until further use. In order to calculate the amount of his-VEGF immobilized onto magnetic MPs, a VEGF ELISA kit (PeproTech EC Ltd., Rocky Hill, NJ, USA) was used according to manufacturer's instructions.

Differentiation of $CD34^+$ cells into OEPCs and preparation of OEPC aggregates. Human umbilical cord blood (UCB) sample collection was approved by the ethical committees of Dr. Daniel de Matos at the Maternity Hospital in Coimbra and the Hospital Infante D. Pedro in Aveiro. Parents signed an informed consent form, in compliance with Portuguese legislation. The $CD34^+$ cells were isolated from human UCB and differentiated into OEPCs as previously described by us[4, 21]. For each experiment, the cells were expanded on 1% (w/v) gelatin-coated T75 flasks (BD Biosciences, Franklin Lakes, NJ, USA) in EGM-2 (Lonza, Gaithersburg, MD, USA) medium.

OEPC aggregates with defined cell numbers were formed as previously reported [22, 23]. Briefly, confluent OEPC cultures were trypsinized and suspended in serum reduced EGM-2 (1% v/v FBS) medium without VEGF and 20% (w/v) methocel. Cells suspended in methocel solution (20,000 cells per 30 µl of methocel solution) were seeded onto nonadhesive bacteriological dishes (Greiner, Frickenhausen, Germany; in drops of 30 µl) and cultured at 37ºC (5% CO_2, 95% humidity) for 12 h. After 12 h, cell aggregates were collected and transferred into untreated 384-well plates (Nunc, Penfield, NY, USA) containing fibrinogen solution. Fibrin gels (30 µl) were prepared by mixing three different components: fibrinogen (10 mg/ml), $CaCl_2$ (Merck, Kenilworth, NJ, USA; 2.5 mM) and thrombin (2 U/ml). This solution was allowed to solidify at 37ºC and 95% relative humidity. After the solidification of the gel, serum-reduced (1% FBS) EGM-2 medium without VEGF was added into each well, on the top of the fibrin gels. The cells were then incubated at 37°C and 5% CO_2 under hypoxia conditions (0.5% O_2) for 24h.

VEGFR-2 phosphorylation studies. OEPCs cultured on gelatin-coated plates were starved in EBM-2 medium without supplements for 20 h, trypsinized and suspended in EBM-2 medium containing MPs or VEGF-MPs at a ratio of 1:2 (cell:particle). The cell suspension

was then seeded as hanging drops in nonadhesive bacteriological dishes (Greiner Bio One Ltd., Gloucestershire, UK) and incubated at 37°C and 5% CO_2 for up to 1 h. After the incubation, the cells were washed with cold EBM-2 medium and collected into pre-chilled centrifuge tubes. Cell suspensions were centrifuged at 1,000 rpm for 3 min at 4°C. The medium was removed immediately, cells were washed with ice-cold PBS containing sodium vanadate (0.2 mM) and incubated on ice with cell lysis buffer for 15 min. Cell lysates were then centrifuged at 2,000 g for 5 min and the supernatants were transferred into clean test tubes. In order to determine the phosphorylation of VEGFR-2 by sVEGF, OEPCs were activated with the same amount of sVEGF for up to 30 min, lyzed and analyzed as described above. Cell lysates were evaluated using phosho and total VEGFR-2 ELISA kits (R&D Systems, Minneapolis, MN, USA) and the ratio of phospho/total VEGFR-2 was calculated according to manufacturer's instructions.

***In vivo* studies**. Mouse experiments are reported in accordance with the Animal Research Report of *In Vivo* Experiments (ARRIVE) guidelines.

Subcutaneous OEPC transplantation in mice. This study was performed in accordance with the Guide for the Care and Use of Laboratory Animals (The Institute of Laboratory Animal Resources, 1996) and approved by the Experimental Animal Committee of MIT. OEPC aggregates containing GFP-expressing OEPCs (1×10^6 cells; Angio-Proteomie, Boston, MA, USA) with or without 1×10^6 MPs were harvested, washed with EC basal medium, centrifuged and mixed in 200 µl fibrinogen (final concentration 10 mg/ml). Thrombin (final concentration 2U/ml) was added to the mixture and the solution rapidly injected subcutaneously on the abdominal midline region of anesthetized nude mice. Mice were imaged under isoflurane anesthesia, by an IVIS® Spectrum *in vivo* imaging system (Xenogen Corporation, Alameda, CA, USA) up to 20 days. IVIS images were taken and analyzed using

Caliper Living Imaging Software. The following parameters have been used: (i) a laser excitation at 490 nm and an emission filter at 510 nm, (ii) an exposure time of 0.5 seconds per image and (iii) an image filed of 12.5 × 12.5 cm. For miRNA isolation, animals were sacrificed 1 day after the surgery and the constructs were collected. The samples were washed with PBS, mounted in OCT compound (VWR, Radnor, PA, USA) and frozen in liquid nitrogen. 20 μm sections were cut using a Leica cryostat and immediately transferred to lysis buffer containing β-mercaptoethanol. The samples were disrupted with 5 mm stainless steel beads (Qiagen, Hilden, Germany) using a Qiagen TissueLyser. miRNA was isolated from the samples using the absolutely RNA miRNA kit (400814, Agilent Technologies, Santa Clara, CA, USA) according to the manufacturer's instructions.

Intramuscular OEPC transplantation in mice with unilateral limb ischemia. Experiments were performed in accordance with the Animal (Scientific Procedures) Act (UK) 1986 prepared by the Institute of Laboratory Animal Resources and performed under UK Home Office Project and Personal License. Experiments were approved by the University of Bristol Ethical Review Committee. Two different groups of OEPCs were transplanted; OEPCs transfected with 50 nM of antagomiR-17 (miRIDIAN Hairpin Inhibitor; Dharmacon Lafayette, CO, USA), or OEPCs transfected with 50 nM antagomiR control (Ambion, Carlsbad, CA, USA). In both groups, antagomiRs were complexed with Lipofectamine RNAiMax (Invitrogen, Carlsbad, CA, USA) and OEPCs were transfected for 48 hours prior to transplantation in mice. Unilateral limb ischemia was achieved by occlusion of the left femoral artery in female CD1 nude mice (age 14 weeks). Immediately after, 3×10^6 cells or their fresh medium vehicle (50 μl of EBM-2) were injected in the ischemic adductor muscle (n=12 mice per group). The superficial blood flow to both feet was measured using high-resolution laser color Doppler imaging system at 30 minutes and days 2, 7, 14, and 21 after limb ischemia. Blood flow recovery was calculated as a ratio of ischemic over contralateral

foot blood flow. After the last Doppler analysis (at day 21 after surgery), mice were sacrificed by perfusion-fixation under terminal anesthesia and limb muscles were harvested for immunohistochemical analyses.

RESULTS

VEGF can be immobilized onto magnetic MPs. VEGF was immobilized onto magnetic MPs (4.5 μm diameter) using biotin-streptavidin chemistry (**Fig. 1A.1**). The biotin-streptavidin system is the strongest noncovalent biological interaction known[24]. In this method, streptavidin-coated MPs were first conjugated with biotinylated anti-histidine antibody, and then, with histidine-tagged VEGF. To determine the success of VEGF immobilization, MPs were separated by a magnet, washed (until no measurable leaching of VEGF was observed), and then exposed to a fluorescent secondary antibody against immobilized VEGF followed by flow cytometry characterization. Streptavidin-coated MPs conjugated with biotinylated anti-his antibody in the absence of his-VEGF showed no fluorescence (**Supplementary Fig. 1A**). In contrast, VEGF-MPs showed an increase in the mean fluorescence indicating that MPs were successfully conjugated with VEGF. Then, we evaluated different initial ratios of anti-VEGF antibody and VEGF to maximize the concentration of immobilized VEGF. Depending on the initial concentrations of antibody and growth factor, the immobilized VEGF amounts were between 271.8±44.3 and 425.4±50.2 ng per 10^6 microparticles (**Supplementary Fig. 1B**). For subsequent studies, MPs conjugated with 425.4±50.2 ng VEGF per 10^6 particles were used.

MPs do not induce toxicity in OEPCs. The toxicity of MPs against OEPCs was determined by cell proliferation, viability and apoptosis assays. Firstly, iron release studies from the MPs were performed by inductively coupled plasma mass spectrometry (ICP-MS). It is known that

MPs might have potential toxic effects especially due to iron release from them[25-27]. Polstyrene-coated MPs were used in our studies to prevent this iron release. Indeed, no significant release of Fe from MPs was determined up to 7 days in cell culture medium at 37°C (**Supplementary Fig. 1C**). In order to evaluate the effect of MPs on cell proliferation, monolayers of OEPCs were used (**Supplementary Fig. 2A**). The cells were treated with different ratios of MPs (1:10-1:100; cell:MP ratios) up to 5 days and cell proliferation quantified by a WST-1 assay. No measurable effect of MPs on cell proliferation was observed (**Supplementary Fig. 2A**). Then, cell viability was monitored in cell aggregates having different cell numbers and cell:MP ratios (**Supplementary Figs. 2B and 2C**). Cell aggregates with small number of cells (≤ 10,000 cells) having a cell:MP ratio of 1:1 showed lower survival than cell aggregates without MPs (**Supplementary Fig. 2B**). Therefore, for subsequent experiments we have used cell aggregates with 20,000 cells having a diameter of approximately 150 μm (**Fig. 1A.3**). Then, we evaluated the cell:MP ratio. Cell aggregates with a cell:MP ratio of 1:1 seem to survive slightly better than the ones with a cell:MP ratio of 1:2 and thus were selected for subsequent experiments (**Supplementary Fig. 2C**). After selection of cell number and cell:MP ratio, we checked whether MPs increased apoptosis in cell aggregates. The MPs did not induce apoptosis in cell aggregates as determined by a TUNEL assay (**Supplementary Fig. 2D**).

VEGF-MPs induce the phosphorylation of VEGFR-2 and increase the cytosolic free Ca^{2+} in OEPCs. The extracellular distribution of VEGFR-2 clusters was initially monitored to evaluate the effect of VEGF-MPs on VEGFR-2. VEGF-MPs induced VEGFR-2 clustering at the cell surface and the clustering was prolonged relatively to sVEGF (**Supplementary Fig. 3A**). To determine the activity of VEGF-MPs, we evaluated the phosphorylation level of VEGFR-2. OEPCs were starved for 20 h, harvested and suspended in basal medium containing either sVEGF or VEGF-MPs. In order to improve cell-MP interaction, the cell

suspension was then seeded in hanging drops and incubated for different period of times (**Fig. 1A.2 and 1A.3**). Cell aggregates without MPs or cell aggregates with uncoated MPs were used as controls. Cell aggregates treated with the same amount of sVEGF showed a rapid increase in the phosphorylation of VEGFR-2 (**Fig. 1B.1**) and returned to its basal level after 10 min. In contrast, cell aggregates with VEGF-MPs showed high levels of VEGFR-2 phosphorylation for at least 30 min (**Fig. 1B.2**).

To confirm that the phosphorylation of VEGFR-2 was mediated by the immobilized VEGF, but not VEGF leaching from the MPs, VEGF-MPs were suspended in cell culture medium at the same concentration used in cell aggregates and incubated at 37°C for 30 min. After incubation, the MPs were removed and starved OEPCs were suspended in MP conditioned medium to generate hanging drops. No increase in VEGFR-2 phosphorylation was observed when MPs conditioned medium was used (**Fig. 1B.2**). These results confirm that the phosphorylation of VEGFR-2 in OEPC aggregates containing VEGF-MPs was mediated by the immobilized VEGF.

Phosphorylation and dephosphorylation of ligated or free VEGFR-2 occurs on the cell surface and in the endosomes[28]. Computational models indicated that Rab4/5 endosomes contain more VEGFR-2 phosphorylated at the Y1175 site while the cell surface has more VEGFR-2 phosphorylated at the Y1214 site[28]. Previously, it was shown that VEGF conjugated onto flat surfaces extended the phosphorylation of the VEGFR-2 at the Y1214 site and activated p38/MAPK pathway[13]. In our study, OEPCs internalize VEGF-MPs (**Supplementary Figs. 3B and 4A**), which may alter the phosphorylation profile of tyrosine residues in VEGFR-2. The phosphorylation of Y1175 and Y1214 peaked after 3-5 min for sVEGF treated group. A similar profile was observed for the phosphorylation of Y1214 in VEGF-MP treated group, while the phosphorylation of Y1175 peaked at 10 min and maintained its levels for additional

50 min (**Supplementary Fig. 5A**). In line with Y1175 phosphorylation results, the phosphorylation of Akt was prolonged in VEGF-MP treated group relatively to sVEGF one (**Fig. 1C.1**). Finally, in agreement with previous studies, p38 phosphorylation was prolonged in VEGF-MP treated group than in sVEGF treated group[13] (**Fig. 1C.2**).

To further evaluate the bioactivity of VEGF-MPs, we assessed their capacity to increase intracellular free Ca^{2+} *via* activation of VEGFR-2[29] (**Fig. 2A**). The phosphorylation of VEGFR-2 activates PLCγ, which in turn activates MAPK/ERK-1/2 pathway and also increases the intracellular levels of Ca^{2+}. In ECs, the initial increase in the cytosolic free calcium is due to Ca^{2+} mobilization from intracellular stores and only afterwards is due to extracellular Ca^{2+} influx[29]. To monitor intracellular levels of Ca^{2+} on single cell level, OEPCs were starved in basal medium without supplements for 20 h and loaded with the calcium-sensitive fluorescent dye Fura-2 AM. Firstly, the cells were activated by sVEGF (**Fig. 2A**). The administration of VEGF induced a fast increase in intracellular free Ca^{2+} uptake after 3 min, peaking at 4-5 min, followed by a decrease in the intracellular Ca^{2+} (6-7 min) and a plateau phase where Ca^{2+} remains constant for the remaining of the experiment (at least 9 min). The rapid response to sVEGF is due to the fast interaction of VEGF with its receptor and the internalization of the receptor-ligand complex[29]. In contrast to sVEGF, VEGF-MPs stimulated the OEPCs continuously for a longer time. In our experiments, changes were followed up to 45 min and an oscillation in Ca^{2+} was observed for the cells stimulated with VEGF-MPs (**Fig. 2A**). Importantly, no changes in the intracellular Ca^{2+} levels were observed for cells exposed to blank MPs. When VEGFR-2 inhibitor Vatalanib was used, the signal was abolished for the cells treated with VEGF-MPs (or sVEGF; data not shown).

Overall, immobilized VEGF, but not sVEGF, prolongs the phosphorylation of VEGFR-2 in OEPCs. This effect seems to be associated with a prolongation in the phosphorylation of

312 tyrosine site Y1175 and the phosphorylation of Akt. In addition, immobilized VEGF prolongs
313 the phosphorylation of p38 as previously reported[13]. The phosphorylation of VEGFR-2 by
314 immobilized VEGF also induced a prolonged accumulation of intracellular levels of Ca^{2+} that
315 were abolished by chemically inhibiting VEGFR-2 with Vatalanib.

316 **VEGF-MPs can enhance the *in vitro* and *in vivo* survival of OEPCs when cultured as cell**
317 **aggregates.** Next, we evaluated whether VEGF-MPs could enhance the survival of OEPCs
318 cultured under hypoxic conditions (0.5% O_2), to mimic the environment that cells encounter
319 after transplantation in ischemic tissues. A suspension of MPs was mixed with a suspension of
320 OEPCs and cell aggregates were formed by a hanging drop methodology[22] (**Fig. 2B**). At 24 h,
321 cell aggregates containing VEGF-MPs showed 60% higher ATP production (and thus
322 indirectly cell viability) than cell aggregates treated with sVEGF (**Fig. 2B.1**). This effect was
323 likely related to the prolonged activation of pro-survival Akt pathway in VEGF-MPs
324 compared to sVEGF groups. Cell aggregates containing VEGF-MPs were also less
325 susceptible to apoptosis. After 12 h (but not at 24 h) of cell aggregate formation, caspase 9
326 activity was lower for the cell aggregates exposed to sVEGF or containing VEGF-MPs than
327 aggregates containing blank MPs (**Fig. 2B.2**). Moreover, TEM results at 24 h confirmed that
328 OEPC aggregates containing VEGF-MPs showed less stress- and cell death-related lipid
329 droplets [15] (**Supplementary Figs. 4B and 4D.1**) and lysosomes [16] (**Supplementary Fig.**
330 **4D.2**) than the ones containing blank MPs or sVEGF (**Supplementary Figs. 4B and 4D**).

331 VEGF-MPs also enhanced the stabilization of vascular networks formed by OEPCs when
332 cultured on top of Matrigel. To evaluate the angiogenic potential of OEPC aggregates with
333 and without VEGF-MPs, cell aggregates were cultured on top of Matrigel under hypoxia
334 (0.5% O_2). The Matrigel assay showed differences in the interaction of VEGF-MPs and blank
335 MPs with OEPCs. Most of the VEGF-MPs were in close contact with OEPCs

(**Supplementary Fig. 5B**), while a significant number of blank MPs were dispersed throughout well and not in the vicinity of sprouting OEPCs. The network length and branching points were then assessed. The highest network length and number of branch points were observed in cell aggregates exposed to sVEGF and VEGF-MPs (**Figs. 2B.3 and 2B.4**). Importantly, the highest long-term stability of the networks was achieved when VEGF-MPs were used. After 60 h, the number of branch points decreased more than 50% for all the conditions, while the decrease was only 30% for cells activated by VEGF-MPs **(Fig. 2B.4)**.

To demonstrate the *in vivo* survival effect of VEGF-MPs, cell aggregates containing 1×10^6 GFP-expressing OEPCs with uncoated MPs, VEGF-MPs or sVEGF were mixed with a fibrin gel precursor solution and injected subcutaneously in mice. OEPC survival was monitored by an IVIS system (**Fig. 3A.1**). Animals treated with the OEPC aggregates containing blank MPs showed a rapid decrease in the fluorescence signal, which was lost at 3 day post-transplantation (**Figs. 3A.1 and 3A.2**). Similarly, animals treated with OEPC aggregates containing sVEGF showed a rapid decrease in the fluorescence signal demonstrating a relatively poor cell survival. However, the animals treated with the OEPC aggregates containing VEGF-MPs showed a fluorescence signal until day 10 supporting the hypothesis that VEGF-MPs improve the survival of transplanted cells.

Overall, *in vitro*, immobilized VEGF enhanced OEPC survival in hypoxia conditions compared to sVEGF. This effect was characterized by a reduction in cell apoptosis as confirmed by a decrease in caspase 9 activity. Our results further indicate that immobilized VEGF has higher *in vivo* pro-survival effect than sVEGF in OEPC aggregates transplanted subcutaneously into nude mice.

Immobilized VEGF modulates the expression of miR-17, miR-217 and miR-222. The miRNA expression profile of OEPC aggregates was determined following 2 h activation

with uncoated MPs, VEGF-MPs or sVEGF by microarray (**Fig. 4A.1**). We further analyzed miRNAs that exhibited a significant expression difference (P<0.05) in OEPC aggregates containing VEGF-MPs relatively to the other groups (including sVEGF) (**Fig. 4A.2, Supplementary Fig. 6 and Supplementary Tables 3-4**). Twenty miRNAs were downregulated in OEPC aggregates containing VEGF-MPs while one miRNA was upregulated (**Supplementary Fig. 6**). We initially focused our attention on hsa-miR-217 and hsa-miR-17, because: 1) they were among the most downregulated miRNAs in cell aggregates containing VEGF-MPs relatively to cell aggregates containing sVEGF (**Supplementary Table 3**), 2) downregulation of hsa-miR-217 and hsa-miR-17 have been associated with the prevention of vascular ageing[30] and enhancement of angiogenic activity[31], 3) qRT-PCR results confirmed that miR-17 and miR-217 were significantly downregulated when the VEGF-MPs were incubated with cells for a short time (2 h) (**Fig. 4A.3**).

Next, we investigated whether a similar trend in the expression of hsa-miR-217 and hsa-miR-17 could be found *in vivo*. Cell aggregates containing 1×10^6 OEPCs were subcutaneously injected in mice and retrieved 1 day after the surgeries (**Fig. 4A.1**). qRT-PCR results showed downregulation of miR-217 expression in both sVEGF and VEGF-MP treated OEPC aggregates compared to OEPC aggregates treated with uncoated MPs. However, miR-17 expression was uniquely downregulated only in the VEGF-MP treated group (**Fig. 4A.4**). Altogether, our results suggest that miR-17 downregulation might be involved in the pro-survival effect of VEGF-MPs in OEPCs. For this reason, we focused our further studies on miR-17.

AntagomiR-17 (amiR-17) increases OEPC survival and angiogenesis by upregulating *CDKN1A*. In order to mimic the downregulation of miR-17 by immobilized VEGF, OEPCs were transfected with amiR-17 using Lipofectamine® RNAiMAX and OEPCs survival was

385 evaluated after 48 h in hypoxic conditions (0.1% O_2). As controls, we used human umbilical
386 vein ECs (HUVECs) to understand whether the effect of amiR-17 was specific to OEPCs or it
387 could be a broader pro-survival molecule for both progenitor and mature ECs, thus increasing
388 the therapeutic potential of VEGF-MPs. MiR-17 downregulation after amiR-17 transfection in
389 OEPCs and HUVECs was confirmed by qRT-PCR (**Supplementary Fig. 7A**). Cell viability
390 assay showed that amiR-17 increased the survival of both cell types in hypoxia (**Figs. 4B.1**
391 **and 4C.1**). Moreover, amiR-17 increased the angiogenic responses in both OEPCs and
392 HUVECs under hypoxic conditions compared to control amiR-treated groups. (**Figs. 4B.2**
393 **and 4C.2**). Next, we investigated whether the aforementioned positive effects of miR-17
394 inhibition in OEPCs were relevant for the therapeutic performance of the cells after their
395 transplantation in mouse ischemic limbs. Indeed, pre-treatment of OEPCs with amiR-17
396 before transplantation accelerated the post-ischemic hemodynamic recovery (**Figs. 5A and B**)
397 and increased the capillary density of ischemic limb 21 days after the surgery (**Figs. 5C-E**).

398 The prevalent function of a miRNA is to inhibit the translation of a series of mRNA targets
399 (usually called miRNA target "genes"). To define the target genes of amiR-17 in OEPCs, we
400 used next generation mRNA sequencing (**Fig. 6A.1, Supplementary Figs. 7B and 7C and**
401 **Supplementary Tables 5-8**). mRNAs that were upregulated by amiR-17 were chosen as
402 direct target genes of the miR-17. These included: 1) *ZNF652* (zinc finger protein 652), which
403 has a tumour suppressive function[21], 2) *SATL1* (spermidine/spermine N1-acetyl transferase-
404 like 1 protein), which has a role in the ubiquitination and degradation of HIF-1a which in turn
405 has a critical role in angiogenesis[32], and 3) *CDKN1A* (cyclin dependent kinase inhibitor 1A,
406 also known as p21), which has a critical role in cell survival[33] (**Fig. 6A.2; Supplementary**
407 **Figs. 7B and 7C**). PCR-based validation confirmed that both *ZNF652* and *CDKN1A*
408 transcripts were up-regulated in OEPCs transfected with amiR-17 vs cells transfected with
409 control amiR. We additionally analyzed previously validated miR-17 targets, although our

sequencing data did not show amiR-17 to significantly alter their expression (**Fig. 6B**). In both OEPCs and HUVECs, downregulation of miR-17 by its inhibitor (amiR-17) significantly increased the expression of several genes, including *CDKN1A*, endothelial differentiation gene *S1PR1*, and *JAK1*, which is important in vascular homeostasis. Next, we investigated whether these changes in gene expression driven by amiR-17 in OEPC could be replicated by treatment with VEGF-MPs. Indeed, as compared to either sVEGF or uncoated MP treated groups, VEGF-MPs upregulated *CDKN1A* in OEPC aggregates both *in vitro* and *in vivo* (**Fig. 6C and 6D**). We additionally confirmed the upregulation of CDKN1A protein in OEPCs following amiR-17 treatment (**Supplementary Fig. 8**). Overall, these results suggest that VEGF-MPs increase the survival of OEPCs by downregulating miR-17 and subsequently upregulating its target genes, particularly *CDKN1A*.

***CDKN1A* and *ZNF652* regulate the pro-survival effect of amiR-17 in OEPCs.** To confirm the direct binding of miR-17 to *CDKN1A* and *ZNF652,* we used a luciferase assay to co-transfected cells with individual 3'-UTR-reporter constructs along with a miRNA-17 mimic (to overexpress miR-17) (**Fig. 7A**)**.** We further tested the functions of CDKN1A and ZNF652 in OEPCs. OEPCs were double-transfected with either *CDKN1A* siRNA, *ZNF652* siRNA, or control siRNA in combination with either amiR-17 or control amiR. The silencing for each target was confirmed at both mRNA (**Supplementary Fig. 9A**) and protein level (**Supplementary Fig. 9B).** The treatment of OEPCs with siRNAs against these gene targets prevented the prosurvival effect that amiR-17 had on OEPC exposed to hypoxia (**Fig. 7B.1 and 7B.2**). In line with these functional data, the gene expression levels of the pro-apoptotic *CASP3* and *CASP9* were decreased by amiR-17, with this response being prevented by concomitant *CDKN1A* silencing (**Supplementary Fig. 10A**). Interestingly, OEPC aggregates containing VEGF-MPs also showed a decrease in these genes both *in vitro* and *in vivo*

435 (**Supplementary Fig. 10B**). Moreover, *CDKN1A* siRNA, but not *ZNF652* siRNA, prevented
436 the *in vitro* angiogenesis response to amiR-17 **(Supplementary Fig. 11)**.

437

438 **DISCUSSION**

439 In this study, we have investigated the pro-survival effect of immobilized VEGF in OEPCs.
440 After demonstrating the bioactivity of immobilized VEGF by phosphorylation of VEGFR-2
441 and induction of the intracellular accumulation of Ca^{2+}, we showed that immobilized VEGF
442 enhanced the survival of OEPCs both *in vitro* and *in vivo*. We have further identified that
443 these positive responses to immobilized VEGF in OEPCs are mediated by a decrease in miR-
444 17, resulting in increased *CDKN1A* (p21) and *ZNF652* expressions **(Fig. 7C)**.

445 We have used the VEGF-MPs to identify molecular targets mediating the prolonged pro-
446 survival effect of immobilized VEGF in OEPCs. Our MP-based system has several
447 advantages over planar surfaces with immobilized VEGF[13, 14, 34]. First, our MPs can be easily
448 conjugated or manipulated by magnetic devices. Second, VEGF-MPs can be incorporated into
449 cell aggregates for *in vivo* transplantation and the downstream targets of VEGF can be
450 evaluated in an *in vivo* setting. Magnetic MPs were chosen in this study because they are
451 easily controlled by a magnet facilitating the synthesis and purification of VEGF-MPs and the
452 characterization of cell aggregates containing VEGF-MPs (removal of the MPs from cell
453 lysates in western blot and RNA isolation studies). To prevent potential toxic effects of these
454 MPs due to iron release[25-27], we have used polystyrene-coated iron oxide MPs. Our results
455 indicate no significant effect in OEPC viability after MP uptake. It was also reported that the
456 injection of high doses of iron (3000 μmol Fe/kg; 168 mg Fe/kg) to rats and beagle dogs did
457 not induce any acute or subacute toxicity[35]. In our study, less than 1 mg Fe/kg mice was
458 injected in animal studies.

Our results indicate that VEGF-MPs induce a prolonged phosphorylation of VEGFR-2 and maintain high intracellular levels of Ca^{2+} as compared to sVEGF. It has been shown previously that the extended phosphorylation on planar surfaces with conjugated VEGF is mediated by the phosphorylation at the site Y1214 of the C-terminal tail of VEGFR-2[13]. Both matrix-bound and soluble VEGF activate several pathways at similar kinetics except for p38. Conjugated VEGF showed higher and prolonged activation kinetics for p38 compared with soluble VEGF[13]. These studies indicated that some pathways are preferentially selected according to the VEGF affinity to the matrix, VEGF presentation and the intracellular trafficking of VEGFR-2[13, 28]. However, due to the internalization of MPs by the OEPCs in our system, the prolonged pY1175 might activate survival pathways, such as Akt. As an expected result of prolonged activity, immobilized VEGF augmented the survival of OEPC aggregates in hypoxia.

Although some biological aspects of immobilized VEGF have been explored, no study targeted the use of immobilized VEGF to improve cell survival both *in vitro* and *in vivo*[13, 14]. Previous studies have shown that VEGF immobilized on different substrates including titanium, fibrin and collagen is superior to sVEGF in promoting EC proliferation [36, 37] and EC branching[25]. In addition, a previous study has shown that VEGF physically immobilized to cell culture substrates could mediate EC survival after exposure to tumstatin, a proapoptotic agent[38]. However, no side-by-side comparison of the prosurvival effect of immobilized VEGF and sVEGF has been done and no *in vivo* prosurvival effect of immobilized VEGF has been reported. In this work, we have demonstrated the prosurvival effect of immobilized VEGF in both *in vitro* and *in vivo*. Subcutaneous injections of cell aggregates containing VEGF-MPs revealed that immobilized VEGF is functional *in vivo* and it enhances cell survival to a greater extent than sVEGF.

For the first time, we have investigated miRNAs as the molecular targets of immobilized VEGF. Our *in vitro* and *in vivo* results show that the dowregulation of miR-17 is important for enhanced OEPC and EC survival. miR-17 was shown to control cellular proliferation and apoptosis by targeting the E2F family of transcription factors[39, 40]. Individual members of miR-17-92a cluster, e.g. miR-17, reduced EC sprouting whereas inhibitors of these miRNAs augmented angiogenesis *in vitro* and *in vivo* by targeting *JAK1*[31]. The JAK/STAT signaling pathway plays a critical role in the vascular homeostasis and disease. Interestingly, the same study showed that inhibition of miR-17 did not affect tumor angiogenesis, indicating a context-dependent regulation of angiogenesis by miR-17 *in vivo*[31]. Our results indicated that another target of miR-17, *CDKN1A*, was significantly upregulated both *in vitro* and *in vivo* when amiR-17 or conjugated VEGF was used. Although CDKN1A is well-known as a cell-cycle inhibitor, it has diverse biological activities such as EC survival and migration[33, 41]. In the literature, it was shown that *CDKN1A* gene transfer prevents apoptosis both *in vitro* and *in vivo*, following the interruption of blood flow[33]. In line, we have showed that the silencing of *CDKN1A* using siRNA reduces amiR-17-mediated OEPC survival and angiogenesis by upregulating apoptosis-related genes such as *CASP3* and *CASP9* and increasing caspase 9 activity. In summary, the present work suggests that immobilized VEGF might increase OEPC survival by downregulating miR-17 and subsequently upregulating *CDKN1A* and *ZNF652*, which are direct target genes of miR-17.

The transcriptional activation of the miR-17-92 cluster upon sVEGF treatment was reported in the literature and the activation of this cluster as a unit was reported to induce proliferation and angiogenic sprouting[20, 42]. However, in these previous studies, the authors did not investigate the function of individual members of this cluster. It is known that miR-17-92a cluster has both pro-angiogenic and anti-angiogenic miRNAs and its regulation of angiogenesis is context dependent[31, 43]. These previous works also showed that the miR-17-

92a cluster activation by sVEGF is time-and cell-dependent[44]. The results show no statistically significant change in the miRNA levels of miR-17-5p after 6h and 12h[44]. This might be the reason why sVEGF does not induce miR-17 expression in our system *in vitro*. The authors also showed that VEGF stimulates the expression of miR-17-92 cluster in human macrovascular venous ECs as well as in mouse microvascular lung ECs, but not in arterial ECs[44]. Overall, context-, cell- and time-dependent regulation of miR-17-92a cluster might explain the differences between our results and these studies.

In conclusion, we show that VEGF-MPs improve the survival and angiogenesis of OEPCs both *in vitro* and *in vivo*. Immobilized VEGF prolonged the VEGFR-2 phosphorylation and Akt signaling up to 1 h, which were diminished in 10 min when sVEGF was used. VEGF-MPs promoted OEPC survival up to 10 days in subcutaneous injections. Our work also reveals that miR-17 is an important molecular target of VEGF-MPs in OEPCs. The downregulation of miR-17 both *in vitro* and *in vivo* is associated with an up-regulation of *CDKN1A and ZNF652* genes. Our study provides novel insights about the molecular mechanism of immobilized VEGF in terms of OEPC angiogenesis and survival.

References

1. Sanganalmath, S.K. & Bolli, R. Cell therapy for heart failure: a comprehensive overview of experimental and clinical studies, current challenges, and future directions. *Circ Res* **113**, 810-834 (2013).
2. Raval, Z. & Losordo, D.W. Cell therapy of peripheral arterial disease: from experimental findings to clinical trials. *Circ Res* **112**, 1288-1302 (2013).
3. Losordo, D.W. & Dimmeler, S. Therapeutic angiogenesis and vasculogenesis for ischemic disease - Part I: Angiogenic cytokines. *Circulation* **109**, 2487-2491 (2004).
4. Pedroso, D.C. et al. Improved survival, vascular differentiation and wound healing potential of stem cells co-cultured with endothelial cells. *PLoS One* **6**, e16114 (2011).
5. Timmermans, F. et al. Endothelial outgrowth cells are not derived from CD133+ cells or CD45+ hematopoietic precursors. *Arterioscler Thromb Vasc Biol* **27**, 1572-1579 (2007).
6. Bompais, H. et al. Human endothelial cells derived from circulating progenitors display specific functional properties compared with mature vessel wall endothelial cells. *Blood* **103**, 2577-2584 (2004).

7. Haider, H. & Ashraf, M. Strategies to promote donor cell survival: combining preconditioning approach with stem cell transplantation. *J Mol Cell Cardiol* **45**, 554-566 (2008).
8. Robey, T.E., Saiget, M.K., Reinecke, H. & Murry, C.E. Systems approaches to preventing transplanted cell death in cardiac repair. *J Mol Cell Cardiol* **45**, 567-581 (2008).
9. Gerber, H.P. et al. Vascular endothelial growth factor regulates endothelial cell survival through the phosphatidylinositol 3'-kinase/Akt signal transduction pathway. Requirement for Flk-1/KDR activation. *J Biol Chem* **273**, 30336-30343 (1998).
10. Yancopoulos, G.D. et al. Vascular-specific growth factors and blood vessel formation. *Nature* **407**, 242-248 (2000).
11. Ferrara, N., Gerber, H.P. & LeCouter, J. The biology of VEGF and its receptors. *Nat Med* **9**, 669-676 (2003).
12. Hawinkels, L.J.A.C. et al. VEGF release by MMP-9 mediated heparan sulphate cleavage induces colorectal cancer angiogenesis. *Eur J Cancer* **44**, 1904-1913 (2008).
13. Chen, T.T. et al. Anchorage of VEGF to the extracellular matrix conveys differential signaling responses to endothelial cells. *J Cell Biol* **188**, 595-609 (2010).
14. Anderson, S.M., Chen, T.T., Iruela-Arispe, M.L. & Segura, T. The phosphorylation of vascular endothelial growth factor receptor-2 (VEGFR-2) by engineered surfaces with electrostatically or covalently immobilized VEGF. *Biomaterials* **30**, 4618-4628 (2009).
15. Lee, S.J., Zhang, J., Choi, A.M. & Kim, H.P. Mitochondrial dysfunction induces formation of lipid droplets as a generalized response to stress. *Oxid Med Cell Longev* **2013**, 327167 (2013).
16. Kirkegaard, T. & Jaattela, M. Lysosomal involvement in cell death and cancer. *Biochim Biophys Acta* **1793**, 746-754 (2009).
17. Losordo, D.W. & Dimmeler, S. Therapeutic angiogenesis and vasculogenesis for ischemic disease - Part II: Cell-based therapies. *Circulation* **109**, 2692-2697 (2004).
18. Catena, R. et al. Increased expression of VEGF(121)/VEGF(165-189) ratio results in a significant enhancement of human prostate tumor angiogenesis. *Int J Cancer* **120**, 2096-2109 (2007).
19. Silva, E.A., Kim, E.S., Kong, H.J. & Mooney, D.J. Material-based deployment enhances efficacy of endothelial progenitor cells. *Proc Natl Acad Sci U S A* **105**, 14347-14352 (2008).
20. Hirschi, K.K., Ingram, D.A. & Yoder, M.C. Assessing identity, phenotype, and fate of endothelial progenitor cells. *Arterioscler Thromb Vasc Biol* **28**, 1584-1595 (2008).
21. Aday, S. et al. Inflammatory modulation of stem cells by Magnetic Resonance Imaging (MRI)-detectable nanoparticles. *RSC Advances* **4**, 31706-31709 (2014).
22. Korff, T. & Augustin, H.G. Integration of endothelial cells in multicellular spheroids prevents apoptosis and induces differentiation. *J Cell Biol* **143**, 1341-1352 (1998).
23. Alajati, A. et al. Spheroid-based engineering of a human vasculature in mice. *Nat Methods* **5**, 439-445 (2008).
24. Holmberg, A. et al. The biotin-streptavidin interaction can be reversibly broken using water at elevated temperatures. *Electrophoresis* **26**, 501-510 (2005).
25. Singh, N., Jenkins, G.J., Asadi, R. & Doak, S.H. Potential toxicity of superparamagnetic iron oxide nanoparticles (SPION). *Nano Rev* **1** (2010).
26. Bishop, G.M. & Robinson, S.R. Quantitative analysis of cell death and ferritin expression in response to cortical iron: implications for hypoxia-ischemia and stroke. *Brain Res* **907**, 175-187 (2001).
27. Riley, M.R., Boesewetter, D.E., Kim, A.M. & Sirvent, F.P. Effects of metals Cu, Fe, Ni, V, and Zn on rat lung epithelial cells. *Toxicology* **190**, 171-184 (2003).

28. Clegg, L.W. & Mac Gabhann, F. Site-Specific Phosphorylation of VEGFR2 Is Mediated by Receptor Trafficking: Insights from a Computational Model. *PLoS Comput Biol* **11**, e1004158 (2015).
29. Dawson, N.S., Zawieja, D.C., Wu, M.H. & Granger, H.J. Signaling pathways mediating VEGF165-induced calcium transients and membrane depolarization in human endothelial cells. *FASEB J* **20**, 991-993 (2006).
30. Menghini, R. et al. MicroRNA 217 modulates endothelial cell senescence via silent information regulator 1. *Circulation* **120**, 1524-1532 (2009).
31. Doebele, C. et al. Members of the microRNA-17-92 cluster exhibit a cell-intrinsic antiangiogenic function in endothelial cells. *Blood* **115**, 4944-4950 (2010).
32. Lee, S., Jilani, S.M., Nikolova, G.V., Carpizo, D. & Iruela-Arispe, M.L. Processing of VEGF-A by matrix metalloproteinases regulates bioavailability and vascular patterning in tumors. *J Cell Biol* **169**, 681-691 (2005).
33. Mattiussi, S. et al. p21(Waf1/Cip1/Sdi1) mediates shear stress-dependent antiapoptotic function. *Cardiovasc Res* **61**, 693-704 (2004).
34. Anderson, S.M. et al. VEGF internalization is not required for VEGFR-2 phosphorylation in bioengineered surfaces with covalently linked VEGF. *Integr Biol (Camb)* **3**, 887-896 (2011).
35. Weissleder, R. et al. Superparamagnetic iron oxide: pharmacokinetics and toxicity. *AJR Am J Roentgenol* **152**, 167-173 (1989).
36. Shen, Y.H., Shoichet, M.S. & Radisic, M. Vascular endothelial growth factor immobilized in collagen scaffold promotes penetration and proliferation of endothelial cells. *Acta Biomater* **4**, 477-489 (2008).
37. Guller, A.E., Grebenyuk, P.N., Shekhter, A.B., Zvyagin, A.V. & Deyev, S.M. Bioreactor-Based Tumor Tissue Engineering. *Acta Naturae* **8**, 44-58 (2016).
38. Hutchings, H., Ortega, N. & Plouet, J. Extracellular matrix-bound vascular endothelial growth factor promotes endothelial cell adhesion, migration, and survival through integrin ligation. *Faseb J* **17**, 1520-1522 (2003).
39. O'Donnell, K.A., Wentzel, E.A., Zeller, K.I., Dang, C.V. & Mendell, J.T. c-Myc-regulated microRNAs modulate E2F1 expression. *Nature* **435**, 839-843 (2005).
40. Pickering, M.T., Stadler, B.M. & Kowalik, T.F. miR-17 and miR-20a temper an E2F1-induced G1 checkpoint to regulate cell cycle progression. *Oncogene* **28**, 140-145 (2009).
41. Bruhl, T. et al. p21Cip1 levels differentially regulate turnover of mature endothelial cells, endothelial progenitor cells, and in vivo neovascularization. *Circ Res* **94**, 686-692 (2004).
42. Fadini, G.P., Losordo, D. & Dimmeler, S. Critical reevaluation of endothelial progenitor cell phenotypes for therapeutic and diagnostic use. *Circ Res* **110**, 624-637 (2012).
43. Bonauer, A. et al. MicroRNA-92a controls angiogenesis and functional recovery of ischemic tissues in mice. *Science* **324**, 1710-1713 (2009).
44. Chamorro-Jorganes, A. et al. VEGF-Induced Expression of miR-17-92 Cluster in Endothelial Cells Is Mediated by ERK/ELK1 Activation and Regulates Angiogenesis. *Circ Res* **118**, 38-47 (2016).

Acknowledgements

We acknowledge the assistance of Dr. Glenn Paradis (MIT, MA, USA) for flow cytometry analyses of the microparticles and Dr. Thomas Kraehenbuehl for his scientific advice. This work was funded by FEDER (Fundo Europeu de Desenvolvimento Regional) through the Program COMPETE and by Portuguese funds through FCT (Fundação para a Ciência e a Tecnologia) in the context of project PTDC/BIM-MED/1118/2012, and by the ERA Chair project ERA@UC (ref: 669088) through European Union´s Horizon 2020 program. S.A. acknowledges doctoral and postdoctoral grants from FCT (SFRH/BD/42871/2008 and SFRH/BPD/105172/2014). C.E. is a BHF Professor in Cardiovascular Science. This study was supported by awards from Leducq Foundation Transatlantic Network on vascular microRNAs, MIRVAD (13 CVD 02) and BHF Regenerative Medicine Centers (RM/13/2/30158).

Author contributions

S.A. designed and performed experiments, analyzed the data and wrote the manuscript. M.B., J.Z., L.C., J.S., and T.S. performed experiments and analyzed the data. L.B. read and corrected the manuscript. R.L. provided research funds, and corrected the manuscript. C.E. provided research funds, analyzed the data and rewrote parts of the manuscript. L.F. provided research funds, designed experiments, analyzed the data, co-wrote the manuscript. All authors approved the final manuscript.

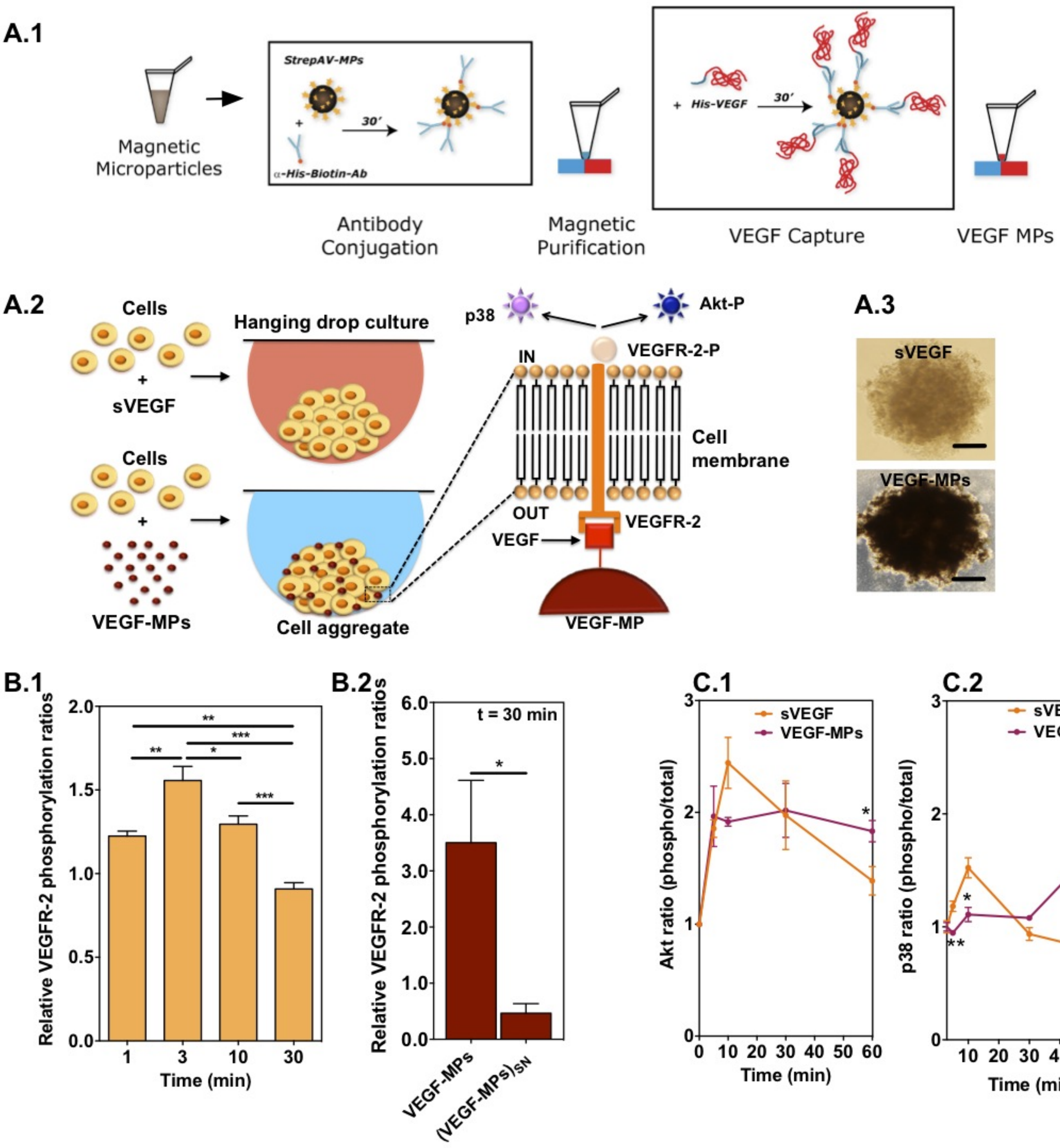

Figure 1. Preparation and biological characterization of VEGF-MPs in OEPCs. (A) Schematic representation of the protocol for the preparation of VEGF-conjugated particles (A.1) and for the formation of cells aggregates containing sVEGF or VEGF-MPs (A.2). (A.3) Light microscopy images of the OEPC aggregates at 24 h. The differences in color of cell aggregates are due to the presence of MPs. Bar corresponds to 50 μm. (B.1) VEGFR-2 phosphorylation in OEPC aggregates cultured in media containing sVEGF. (B.2) VEGFR-2 phosphorylation in OEPC aggregates containing VEGF-MPs or containing cell culture media exposed to the same number of MPs used to make the cell aggregates [$(VEGF\text{-}MPs)_{SN}$]. VEGF phosphorylation was quantified by ELISA. Values are given as average ± SEM (n=4-8). (C) ELISA quantification of phospho-Akt/total Akt (C.1) and phospho-p38/ total p38 (C.2). Values are given as average ± SEM (n=3). $P \leq 0.05$ (*), $P \leq 0.01$ (**), $P \leq 0.001$ (***) and $P \leq 0.0001$ (****).

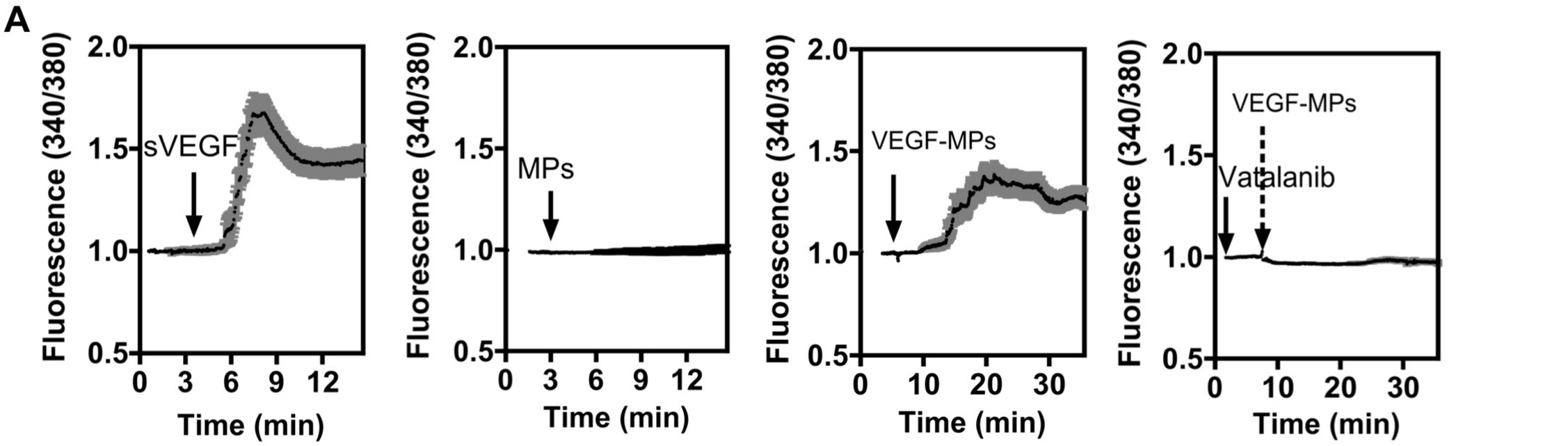

Figure 2. The biological effect of VEGF-MPs on OEPCs. MPs indicates cell aggregates containing uncoated beads while $(VEGF\text{-}MPs)_{SN}$ indicates cell aggregates exposed to the supernatant of VEGF-MPs. (A) Single cell calcium measurements. OEPCs were starved in medium without serum for 20 h, loaded with a Ca^{2+} probe and activated by VEGF, blank MPs, VEGF-MPs or inhibited by Vatalanib, an inhibitor of VEGFR-2. The arrows indicate the time when the compounds or MPs were added. At least 10 cells have been monitored for intracellular Ca^{2+} in each of the experimental groups. Averages and SEM values are in black and grey, respectively. (B) Schematic representation of the protocols used to demonstrate the higher OEPC survival and activity after exposure to VEGF-MPs than sVEGF. (B.1-B.2) The survival (B.1; 24 h) and apoptosis (B.2; 12 and 24 h) of OEPCs in aggregates under hypoxia in serum-deprived conditions and hypoxia as assessed by an ATP-based assay or the measurement of caspase 9 activity. (B.3-B.4) OEPC aggregates were cultured on Matrigel under hypoxia for 12 and 60 h, after which the tube length (B.3) and branching points (B.4) were measured. In all graphs, values are given as average ± SEM (n=3-8). $P \leq 0.05$ (*), $P \leq 0.01$ (**), $P \leq 0.001$ (***) and $P \leq 0.0001$ (****).

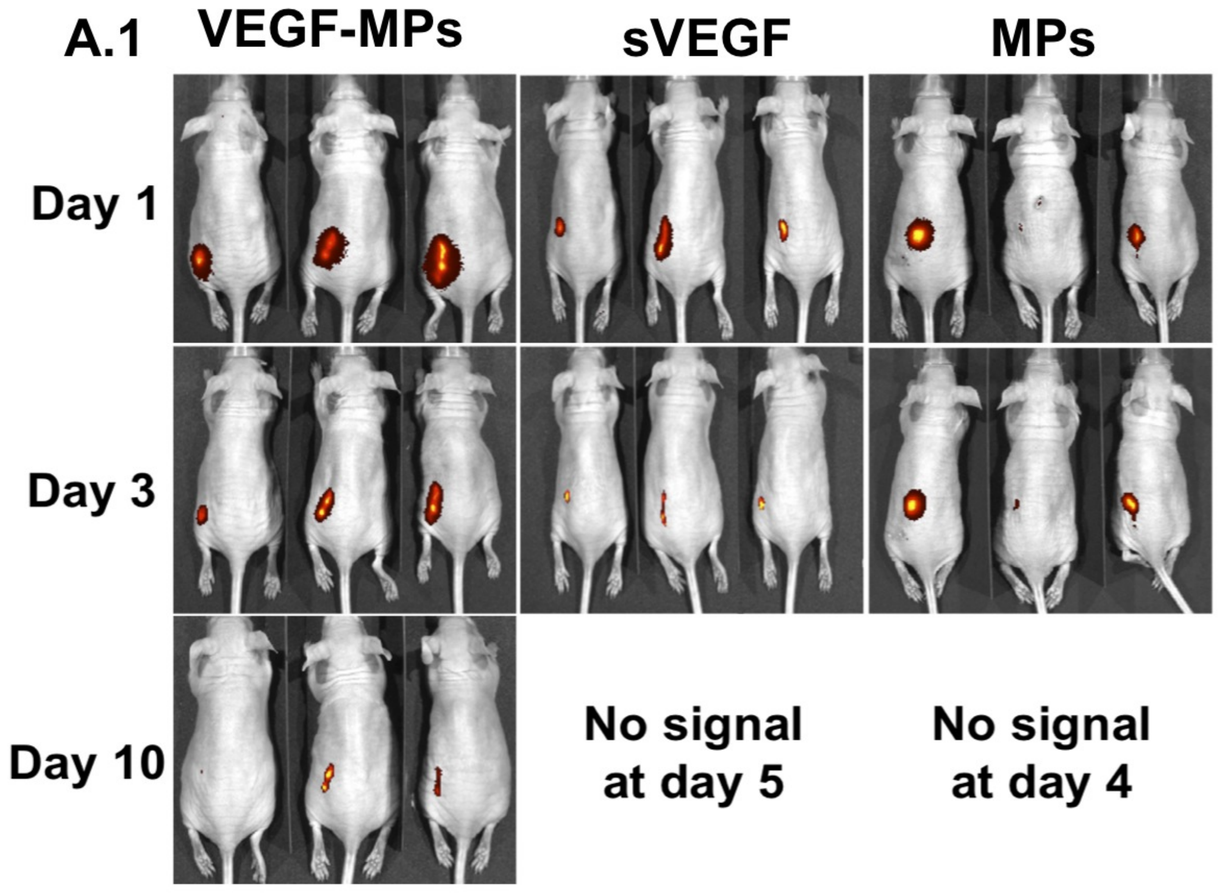

Figure 3. OEPC aggregates containing VEGF-MPs have improved *in vivo* survival after subcutaneous injections. OEPC aggregates were prepared with sVEGF, non-coated MPs or VEGF-MPs. (A.1) Representative IVIS images and (A.2) fluorescence intensity measurements of mice following injection of cell aggregates containing 1 million GFP-labeled OEPCs with sVEGF, blank MPs or VEGF-MPs. The fluorescence intensities were normalized by day one. Results are average ± SEM (n=7).

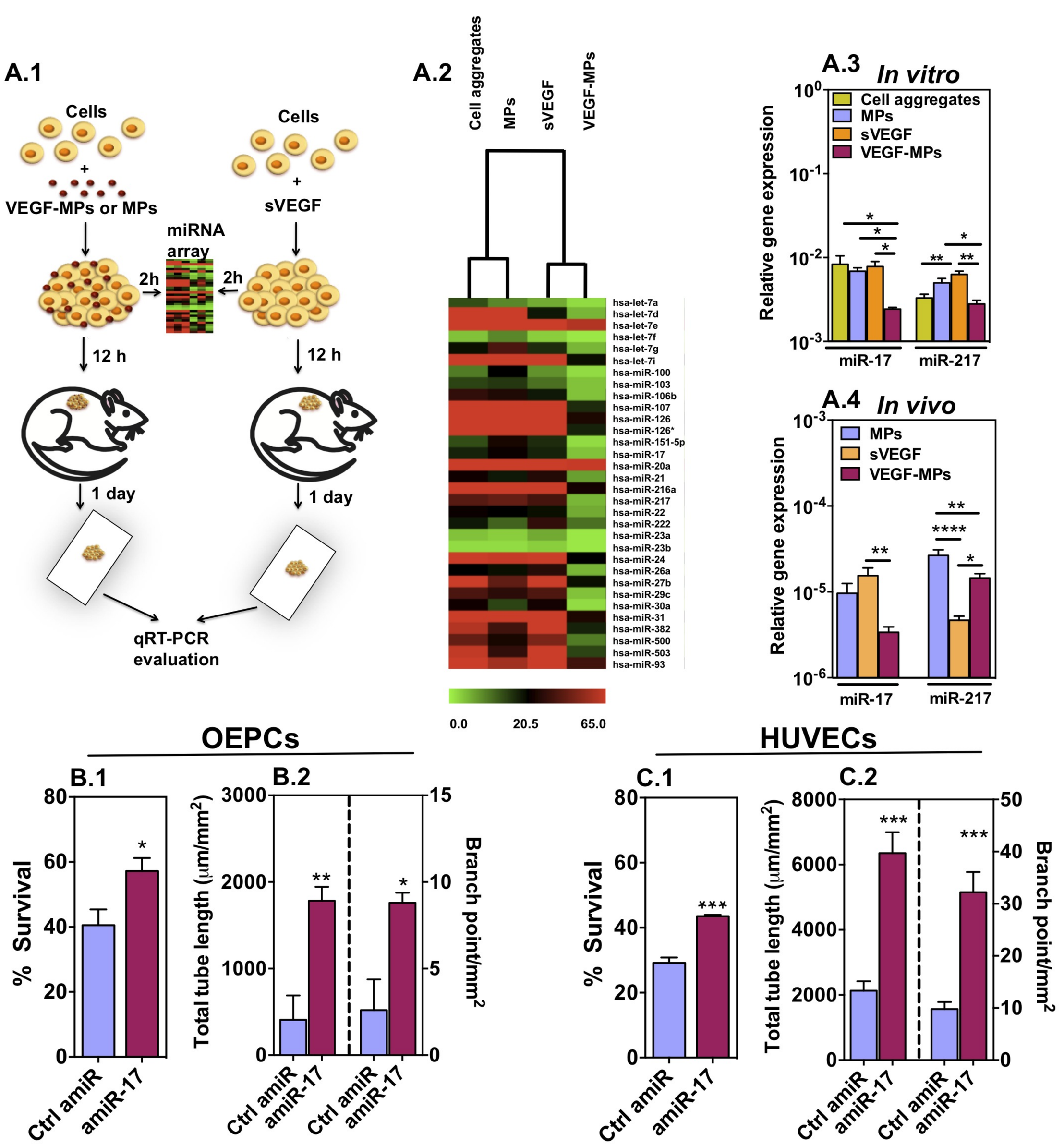

Figure 4. Identification of a miRNA associated with the pro-survival and function of OEPCs after contact with VEGF-MPs. (A.1) Schematic representation of the protocol used to identify miRNAs mediating the effect of VEGF-MPs. (A.2) Differentially regulated miRNAs (P<0.005) in OEPC aggregates cultured *in vitro* for 2 h as evaluated by miRNA array. (A.3) Validation of some miRNAs by qRT-PCR. (A.4) miRNA expression as evaluated by qRT-PCR in OEPC aggregates implanted subcutaneously in mice for 1 day. U6 was used to normalize the data. In all graphs, values are given as average ± SEM (n=3-4). P ≤ 0.05 (*), P ≤ 0.01 (**) and P ≤ 0.001 (***). (B.1 and C.1) Survival of OEPCs (B.1) or HUVECs (C.1) transfected with control antagomiR (Ctrl amiR) or antagomiR-17 (amiR-17), in serum-deprived conditions for 48 h under hypoxia conditions (0.1% O_2), as assessed by Presto Blue assay. (B.2-C.2) Transfected OEPC or HUVECs with Ctrl amiR or amiR-17 were cultured on Matrigel for 48 h under hypoxia after which the tube length and branching points were measured. In all graphs, values are given as average ± SEM (n=4). P ≤ 0.05 (*), P ≤ 0.01 (**) and P ≤ 0.001 (***).

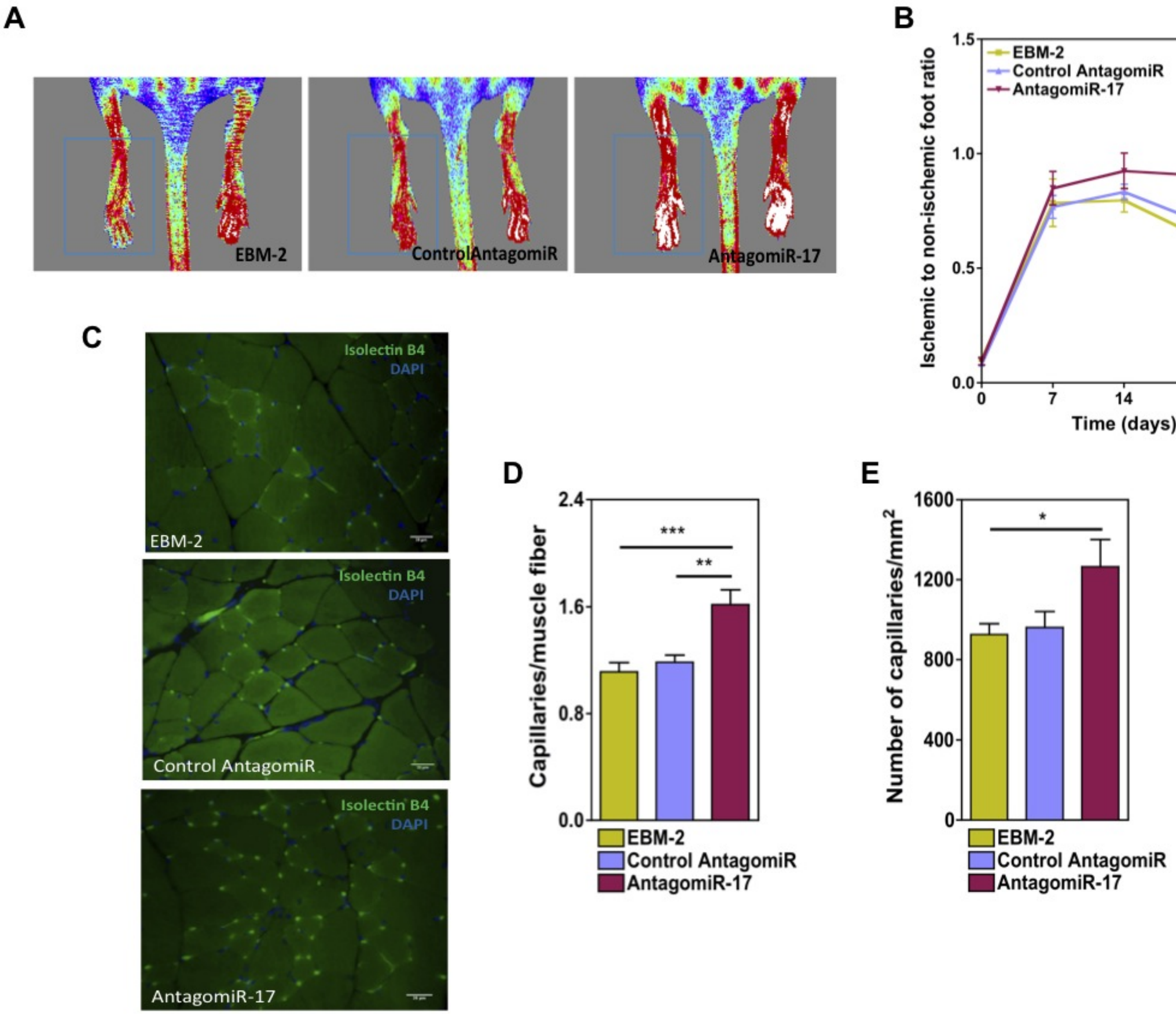

Figure 5. AntagomiR-17-treated OEPCs significantly increase the post ischemic blood flow recovery and capillary density in a mouse model of hindlimb ischemia. (A-B) Unilateral limb ischemia was induced in female CD1 nude mice by occlusion of the left femoral artery. Immediately after occlusion, the ischemic muscles were injected with 3 million antagomiR-17-transfected OEPCs or 3 million control antagomiR-transfected OEPCs. Control group received only EBM-2. Blood flow recovery was measured using high resolution laser color Doppler imaging and calculated (n = 12 mice/experimental group) as a ratio of ischemic over contralateral foot blood flow. (C-E) 21 days after surgery, limb muscles were harvested and prepared for immunohistochemical analyses. Capillary density in the adductor muscle was measured by staining with isolectin B4 (revealing endothelial cells) (C). The relative amount of positive cells was counted in 8 randomly selected high-power fields (magnification 20X) (D-E). Data were shown as mean±SEM. $P \leq 0.05$ (*), $P \leq 0.01$ (**) and $P \leq 0.001$ (***).

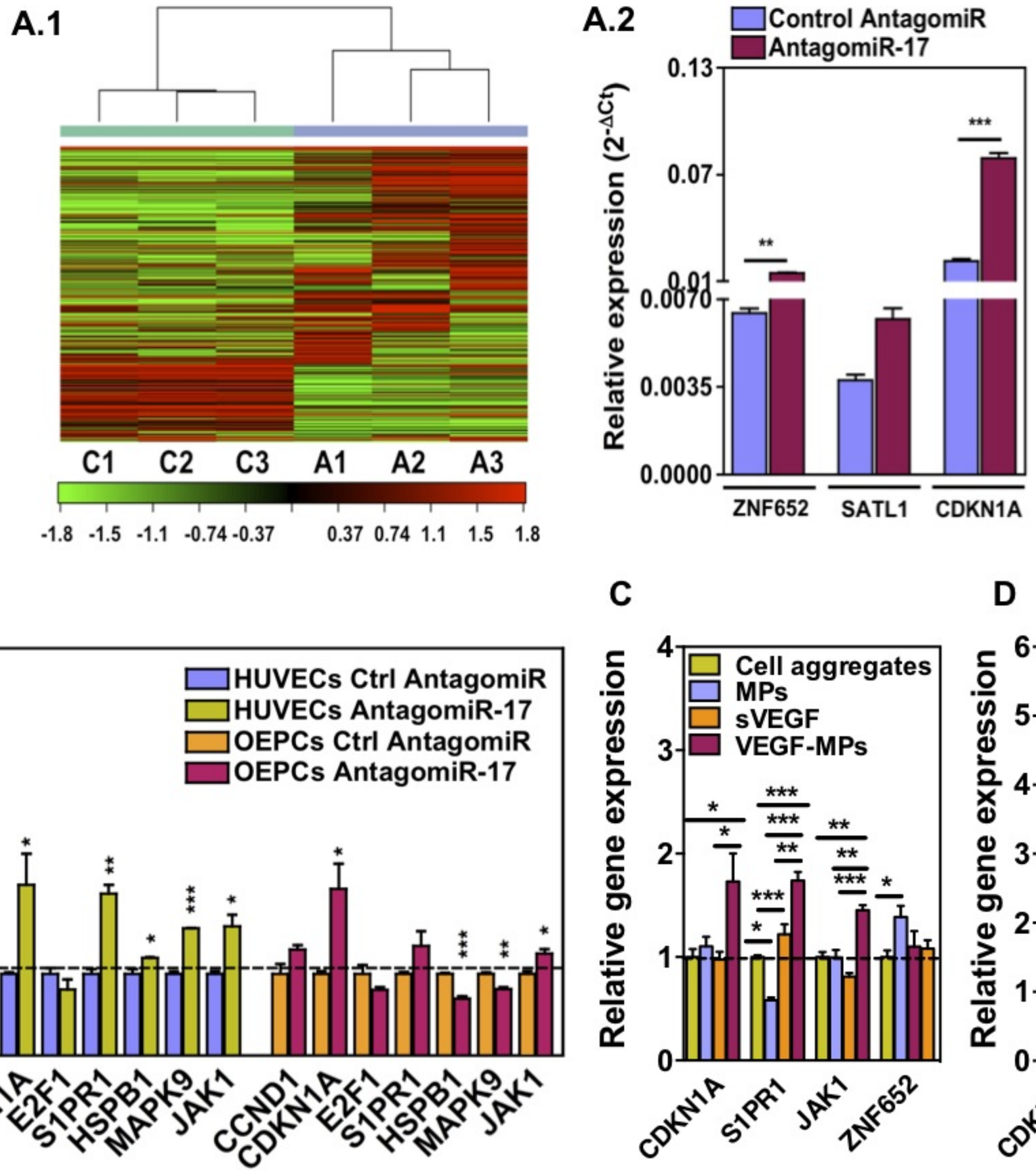

Figure 6. Gene targets of miR-17 in OEPCs. (A) mRNA sequencing was performed for OEPCs transfected with control antagomiR or antagomiR-17 for 48 h. (A.1) The heat map diagram showing the result of the two-way hierarchical clustering of RNA transcripts and samples, by including the top 500 transcripts (genes) that have the largest log2 fold difference based on FPKM counts. Each row represents one RNA transcript and each column represents one sample. The color of each point represents the relative expression level of a transcript across all samples. The color scale is shown at the bottom right: red represents an expression level above the mean; green represents an expression level below the mean. On heat map, C is control amiR while A is amiR-17. (A.2) Validation of 3 gene targets by qRT-PCR. (B) The expression of previously reported miR-17 gene targets in HUVECs and OEPCs transfected with amiR-17. The results were normalized to control amiR group for each gene. Among the genes tested, CDKN1A was significantly upregulated in both of the cell types transfected with amiR-17. The upregulation in the expression of CDKN1A was also confirmed in OEPCs aggregates containing conjugated VEGF both in 24 h in vitro (C) and 24 h in vivo (D) samples. The gene expression results were normalized to cell control group (cell aggregates). Results are average ± SEM (n=4-8). $P \leq 0.05$ (*), $P \leq 0.01$ (**) and $P \leq 0.001$ (***).

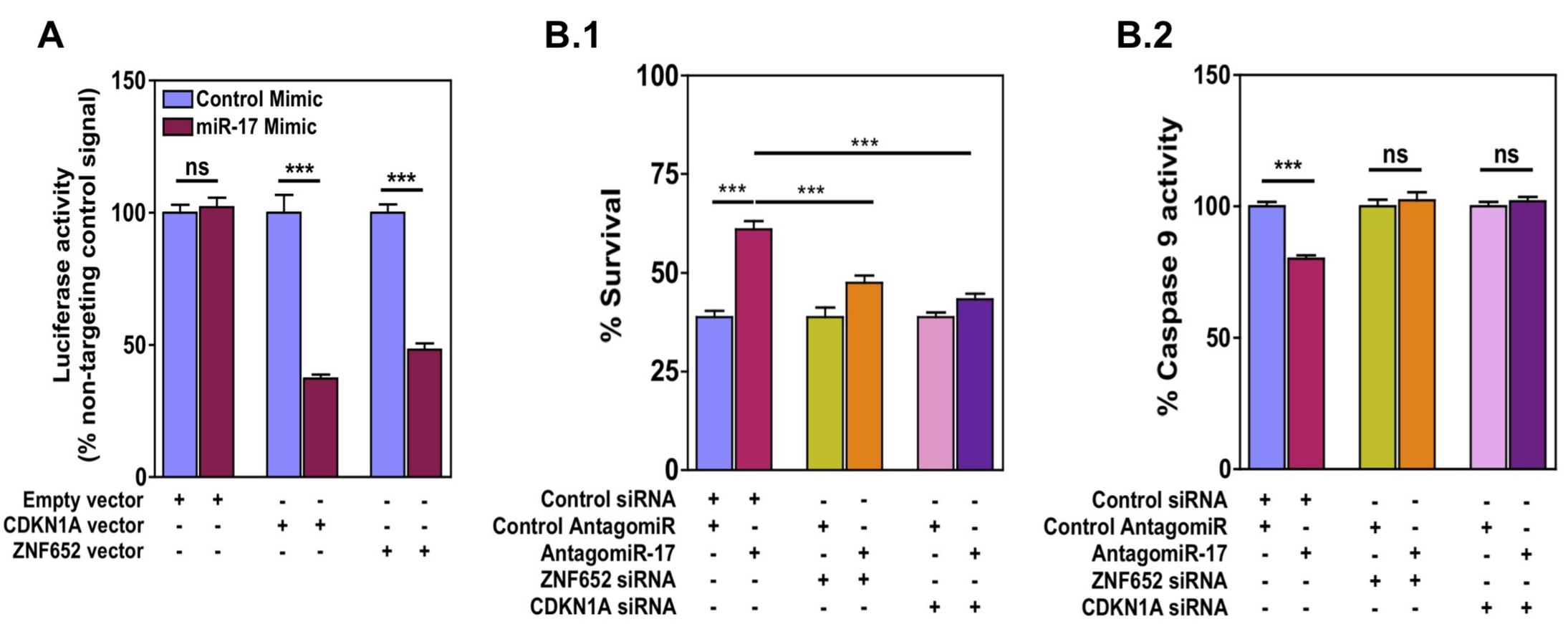

Figure 7. AmiR-17 exerts its pro-survival effect by upregulating CDKN1A. (A) HEK293 cells were double transfected with 100 ng of each 3´UTR luciferase reporter vectors (empty vector, CDKN1A vector or ZNF652 vector) and 50 nM miRNA mimics (control miRNA or miR-17). Signals from 3´UTR reporters for the CDKN1A and ZNF652 genes were significantly knocked down when co-transfected with miR-17, but not with control miRNA. No difference between control miRNA and miR-17 was observed when the empty vector was used. (B) OEPCs cultured in monoculture were silenced for *ZNF652* and *CDKN1A* genes by the use of siRNA. After 2 days of transfection, OEPCs were washed and the cell culture medium was replaced by EBM-2 and cells were incubated under hypoxia conditions (0.1% O_2), with 5% CO_2. After 48 h, both cell survival (by a Presto Blue cell viability assay; B.1) and cell apoptosis (B.2) were evaluated. In A and B, the values are given as average ± SEM (n=10). $P \leq 0.05$ (*), $P \leq 0.01$ (**) and $P \leq 0.001$ (***). (C) Schematic representation of the action mechanism of the VEGF-conjugated microparticles used in this study. The interaction of conjugated VEGF with VEGFR-2 prolongs the phosphorylation of the receptor, calcium signaling and Akt phosphorylation compared with soluble VEGF group. Conjugated VEGF also downregulates miR-17, which leads to the upregulation of CDKN1A expression. Activation of Akt and downregulation of miR-17 lead to an increase in cell survival by reducing apoptosis and favors sprout formation.